REAL TIME ADAPTIVE ULTRASOUND SPECKLE REDUCTION AND COHERENCE ENHANCEMENT

Khaled Z. Abd-Elmoniem, Yasser M. Kadah, and Abou-Bakr M. Youssef
Department of Systems and Biomedical Engineering
Cairo University
Cairo, Egypt

ABSTRACT

We present a novel approach for speckle reduction and coherence enhancement of the ultrasound images. The algorithm maximally low-pass filter those parts of the image which correspond to fully developed speckle, while substantially preserving information associated with resolved-object structure. The proposed algorithm is based on coherent anisotropic diffusion with an efficient discretization scheme that could be used as a preprocessing step for online visualization of ultrasound images even when it is implemented on a PC based system. It is shown experimentally that this technique produced superior results when compared to results obtained from similar methods.

Keywords- Nonlinear anisotropic diffusion, ultrasound image, speckle reduction, coherence enhancement.

1. INTRODUCTION

Noise and artifacts can cause signal and image degradations for many medical imaging modalities. Different image modalities exhibit distinct types of degradation. Radiographs often exhibit low contrast while images formed with coherent energy, such as ultrasound, suffer from speckle noise.

The noninvasive nature, low cost, portability, and real-time image formation make ultrasound imaging an attractive tool for medical diagnosis. One of the limitations of ultrasound images is poor image quality affected by speckle noise. Speckle reduction remains a difficult problem due to the lack of reliable models to estimate noise.

Image degradation can have a significant impact on image quality and thus affect human interpretation and the accuracy of computer-assisted methods. Poor image quality often makes feature extraction, analysis, recognition, and quantitative measurements problematic and unreliable. The denoising and feature enhancement developed in this study may help to improve the accuracy and reliability of image processing algorithms targeting both quantitative and qualitative problems. It is now agreed by many authors that it would be desirable to remove, or reduce the speckle in pulse-echo images, since its presence degrades the apparent resolution in the image to a point below the diffraction-predicted value and it interferes with the visual assessment of small differences in mean gray level or texture.

A number of methods have been suggested for achieving this, most of methods involving temporal averaging, median filtering, maximum amplitude writing (temporal dilation), adaptive speckle reduction (ASR), Wiener filtering, and wavelet shrinkage. Temporal averaging and multi-frame methods try to increase SNR by generating multiple uncorrelated images that are summed incoherently to reduce speckle. These approaches suffer from two drawbacks. First, to produce uncorrelated images the transducer has to be translated at least by about half its width multiplied by the number of the generated frames. Second, temporal averaging based on transducer movement destroys small details such as small vessels, and texture patterns that will be inevitably blurred. On the other hand, Adaptive speckle unsharp filter [2][6] depends on SNR to permit a variant degree of smoothing according to the extent of the speckle pattern from the fully formed speckle (FFS). This approach works well when applied on the uncompressed backscattered envelope signal but greatly suffer from inaccuracy with the log-compressed one. Besides, Wavelet shrinkage method seems to be applicable only off-line. The algorithms above do not seem to have a coherence enhancing criteria.

We describe a new method by which ultrasound pulse-echo image be smoothed to suppress the FFS, while substantially preserving the image component corresponding to resolved (or partially resolved) object structure. This method is based on the nonlinear diffusion model adapted to remove the compressed speckle pattern form the sticks of the convex array B-mode ultrasound images. The choice of sticks instead of the formed image is motivated by two reasons; First, it is clearly more accurate since the actual scan is rather in radial coordinates than in Cartesian coordinates. Second, it is nearly six times as fast as when it is applied on the whole formed image. Besides, the model allows, due to its anisotropy, coherent structure enhancement.

The paper is organized as follows; Section two presents a review of ultrasound speckle properties and the effect of compression while a summary on nonlinear diffusion model is described in the section two. System model is detailed in section three. Section four presents experimental results both on phantoms and actual clinical images. Section five includes the discussion as long as the final conclusion.

0-7803-6297-7/00/$10.00 © 2000 IEEE

2. SPECKLE MODEL

2.1 Medical ultrasound speckle pattern

The nature of speckle pattern depends mainly on the number of scatterers per resolution cell or Scatterer Number Density (SND) and their spatial distribution and the characteristics of the imaging system itself it can be divided into three main classes:

(a) The fully formed speckle pattern occurs when many fine randomly distributed scattering sites exist within the resolution cell of the imaging system (SND > 10) in which the amplitude of the backscattered signal can be modeled as a Rayleigh distributed random variable with a constant SNR of 1.92. Under such conditions the speckle pattern represents a signature of the imaging instrument [2]. Blood cells are a typical example.

(b) The second class of tissue scatterers is nonrandomly distributed with long-range order [1]. Examples of this type are the lobules in liver parenchyma. It contributes a coherent or specular backscattered intensity that is itself spatially variant. The pattern is associated with an the effective number of scatterers is finite (SND < 10). This situation is modeled by K distribution and is associated with (SNR < 1.92) [6].

(c) The third class occurs when a spatially invariant coherent structure is present within the random scatterer region such as organ surfaces and blood vessels [1]. The probability density function (PDF) of the backscattered signals becomes Rician distribution. This class is associated with (SNR > 1.92) [6].

From this summary we discover that the coherence phenomena make SNR an ambiguous feature and cannot be used alone. The deviation in the image properties due to the presence of coherent structures 'partially or completely resolved' results in a speckle pattern which is no longer entirely characteristic of the imaging system [2]. It should therefore be possible to use these deviations to classify each local region of the image according to how much it resembles the fully formed speckle normally generated by that particular imaging system in that part of the image. This measure of similarity can then be used to control the spatial bandwidth of a smoothing filter of some kind, so that regions of the image which closely resemble the fully formed speckle are replaced by a local mean value and, at the other extreme, regions with properties which are least similar to fully formed speckle are not smoothed [2].

2.2 Effect of logarithmic compression

Due to the limited dynamic range of commercial display monitors, ultrasound imaging systems compress the echo signal to fit in the display range. This compression changes the characteristics of the signal PDF. The compression affects the high intensity tail of the Rayleigh and Rician PDF more than its effect on the low intensity part such that the signal is now very close to be with additive Gaussian noise corresponding the uncompressed Rayleigh signal [6].

3. MATERIALS AND METHODS

3.1 Relation to previous work

SNR remains the most fundamental feature that is most widely used in single feature texture classifiers due to its sensitivity to the variation of scatterer distribution in a region. The unsharp filter, described in [2], allowed a degree of smoothing controlled by the local features of image texture and was concerned with differentiating FFS pattern from class two pattern therefore, took the form::

$$\hat{x} = \bar{x} + k(x - \bar{x}) \qquad (1)$$

where $\hat{x}$ is the new (processed) value of a pixel to be computed from the old unprocessed value, x , and the local mean of the old values surrounding and including that pixel, $\bar{x}$. The constant, k, is controlled by the measure of similarity p , which in this case is the deviation in the ratio of the local variance of gray levels to the local mean;

where $\bar{p}_s$ is the mean value of p in a region corresponding to fully formed speckle [2].

3.2 Nonlinear Anisotropic Diffusion

Diffusion algorithms remove noise from an image by modifying the image via a partial differential equation (PDE). For example, consider applying the isotropic diffusion equation (the heat equation) given by $\partial I(x, y, t)/\partial t = \mathrm{div}(c\nabla I)$, using the original (degraded / noisy) image $I(x, y, 0)$ as the initial condition, where $I(x, y, 0): \Re^2 \rightarrow \Re^+$ is an image in the continuous domain, (x,y) specifies spatial position, t is an artificial time parameter, c is the diffusion constant, and where ∇I is the image gradient. Modifying the image according to this linear isotropic diffusion equation is equivalent to filtering the image with a Gaussian filter.

The previous model can be put in the form:

$$x_{i+1} - x_i = (1-k)(\bar{x}_i - x_i) \qquad (2)$$

which is very close to the nonlinear isotropic diffusion model

$$I_{t+1} - I_t = g(p)(I_{\sigma xx} + I_{\sigma yy}) \qquad (3)$$

where I_σ is the ultrasound image after averaging with a linear Gaussian kernel of scale σ. g(p) is a function of the SNR or $g = \bar{p}_s / p$ which represent a nonlinear diffusivity replacing the constant diffusivity in the linear case. Diffusion is maximum (g=1) in Rayleigh scatterer region and zero in a fully structured or correlated region (specified experimentally for each imaging system environment).

Simple speckle reduction algorithms like the model above enhance only region associated with a decreasing SNR i.e.

class two while organ surfaces are missclassified and possibly derogated.

3.3 Original formulation

Perona and Malik [3] replaced the classical isotropic diffusion with

$$\partial I(x,y,t)/\partial t = div[g(\| \nabla I \|) \cdot \nabla I] \qquad (4)$$

where $\| \nabla I \|$ is the gradient, and $g(\| \nabla I \|)$ is the diffusivity function or the edge-stopping function [4]. This function is chosen to satisfy $g(x) \to 0$ when $x \to \infty$ and is monotonically decreasing so that the diffusion or the smoothing decreases as the gradient strength increase and the diffusion is stopped across edges.

3.4 Coherent Nonlinear Anisotropic Diffusion

Although g(x) can be a scalar function and diffusion is still anisotropic but since ∇I serves only as an edge detector, the applicability of the above filter is restricted to smoothing with edge enhancement. In general g(x) can be in a tensor form that measures local coherence of structures such that the diffusion process become more directional in both the gradient the contour directions, the directions of maximum and minimum variations respectively.

The coherent diffusion model takes the form

$$\partial I(x,y,t)/\partial t = div[D \nabla I] \qquad (5)$$

where $D \in \Re^{2\times 2}$ is a symmetric positive semi-definite diffusion tensor representing the required diffusion in both gradient and contour directions and hence enhancing coherent structures as well as edges.

There are two tensors widely used to detect the local coherence; the structure tensor (also called scatter matrix or (windowed second) moment tensor) and the Hessian tensor which represents the second order derivatives.

$$\underbrace{\begin{pmatrix} I_x^{\,2} & I_x I_y \\ I_x I_y & I_y^{\,2} \end{pmatrix}}_{\text{Structure matrix}} \qquad \underbrace{\begin{pmatrix} I_{xx} & I_{xy} \\ I_{xy} & I_{yy} \end{pmatrix}}_{\text{Covariance (Hessian) matrix}}$$

Because the Hessian matrix is more sensitive to noise, we preferred to use the structure tensor.

The multiscale structure matrix takes the form

$$J_\rho(\nabla I) = K_\rho * (\nabla I \otimes \nabla I) = K_\rho * (\nabla I \cdot \nabla I^T) \qquad (\rho \geq 0)$$

where $$K_\sigma(x) = (2\pi\sigma^2)^{-1} \cdot \exp(|x|^2 / 2\sigma^2)$$

The convolution above is done component-wise mainly to average a feature over a known neighborhood (scale) where ρ is the integration scale (the window size) over which the orientation information is averaged [5]. The eigenvectors w_1, w_2 and the eigenvalues μ_1, μ_2 correspond to the directions of maximum and minimum variations and the strength of these variations respectively.

4. COHERENT FILTERING MODEL

4.1 Proposed model description

The diffusion tensor D should be chosen with the same eigenvectors of the structure matrix but with eigenvalues that represent the strength of diffusion in each principal direction.

$$\text{Let } J_\rho(I) = \begin{pmatrix} K_\rho * I_x^2 & K_\rho * (I_x I_y) \\ K_\rho * (I_x I_y) & K_\rho * I_y^2 \end{pmatrix}$$

$$\text{Then } D(I) = \begin{pmatrix} w_1 & w_2 \end{pmatrix} \begin{pmatrix} \lambda_1 & 0 \\ 0 & \lambda_2 \end{pmatrix} \begin{pmatrix} w_1^T \\ w_2^T \end{pmatrix}$$

$$\text{Where } \lambda_1 = \begin{cases} \alpha \cdot \left(1 - (\mu_1 - \mu_2)^2 / s^2\right) & \text{if } (\mu_1 - \mu_2)^2 \leq s^2 \\ 0 & \text{else} \end{cases}$$

$$\lambda_2 = \alpha$$

4.2 Discretization scheme

Due to the need for I_{xx}, I_{yy}, and I_{xy}, all the 8-points neighborhood are used in the model therefore explicit scheme seems stable for only very small step (Δt <1/4 for the scalar diffusion) [5] and even smaller for this model. Implicit scheme is extremely complicated due to the nonlinearity and the bulky system matrix to be solved. Although semi implicit has shown unconditional stability in scalar nonlinear diffusion for any time step where the system matrix is divided into two simple tridiagonal ones but in this coherent model the scheme is no longer simple due to the added diagonal points. For these reasons and since we are concerned with fast implementation, we thought of a hybrid scheme that combines two important features; stability and fastness.

The scheme can be summarized as follows:

$$I_{i,j}^{t+\Delta t} \Leftarrow \begin{pmatrix} I_{i-1,j+1}^{t} & I_{i,j+1}^{t+\Delta t} & I_{i+1,j+1}^{t} \\ I_{i-1,j}^{t+\Delta t} & I_{i,j}^{t} & I_{i+1,j}^{t+\Delta t} \\ I_{i-1,j-1}^{t} & I_{i,j-1}^{t+\Delta t} & I_{i+1,j-1}^{t} \end{pmatrix}$$

where $I_{i,j}^{t}$ stands for the pixel at location x=i, y=j at time instance t. In this scheme splitting can be used to convert the system matrix into two tridiagonal matrices which are easily solved.

5. RESULTS AND DISCUSSION

Several reasons are behind choosing this model:

(a) Our main objective is to produce a filter not only an edge preserving but also a coherence enhancing to overcome the ambiguity of using the SNR alone and to further enhance both tissue texture, organ surfaces, and blood vessels.

(b) λ_1 is related to the anisotropy of the image $(\mu_1 - \mu_2)$ through a monotonically decreasing function that resemble Tukey's biweight robust estimator which preserves sharp boundaries and improves the automatic stopping of the diffusion in the gradient direction [4].

(c) The stopping level s^2 is determined experimentally corresponding to the fully structured region.

The model is applied on the ultrasound convex B-mode sticks, 80 sticks of 320 samples each. Since, the sticks coordinates are closer to radian than to the Cartesian, the model is modified simply by adjusting the gradient step in the axial direction to take into consideration the diverging pattern of the sticks. The benefit of using the sticks before scan conversion is very clear; the small number of pixels makes the algorithm at least three times faster, the algorithm is now more accurate since the coordinate system is the same as that of the probe.

Fig.1 illustrates the results of applying the proposed algorithm to standard phantom with positive and negative contrast regions. Fig.2 shows the effect on standard clinical images. Applying two iterations each of $\Delta t = 2$, $\alpha = 0.9$ and $s^2=2$. It is apparent that speckle suppression while preserving and even enhancing coherent structures has been achieved to a great extent. We expect that area calculations of heart chambers and urinary bladders are now more robust. Although the algorithm was not implemented optimally yet we reached a rate of 70msec/ iteration on a PC with PII 366 MHz microprocessor which is suitable for real time processing.

6. CONCLUSION

We introduced a coherent diffusion model to reduce ultrasound speckle while preserving the appearance of structured regions and organ surfaces. Thanks to its robustness of parameter selection; the algorithm is suitable for commercial implementation. Texture and organ surfaces have been enhanced and even the disrupted regions due to ultrasound behavior have been reconnected again. We are now concerned with the effect of this algorithm on the automatic detectability of liver and breast abnormalities and how could the parameters be calculated automatically.

7. REFERENCES

[1] R.F. Wagner, M.F. Insana, " Analysis of ultrasound image texture via generalized Rician statistics, " *Proc. SPIE 556*,pp. 153-159,1985.

[2] J.C. Bamber and C. Daft, " Adaptive filtering for reduction of speckle in ultrasound pulse-echo images, " *Ultrasonics*, pp. 41-44, Jan. 1986.

[3] P. Perona and J. Malik, " Scale space and edge detection using anisotropic diffusion, " *IEEE Trans. PAMI*, vol. 12, pp. 629-639, 1990.

[4] M. J. Black, G. Sapiro, D.H. Marimont, and D. Heeger, " Robust anisotropic diffusion, " *IEEE Trans. Imag. Proc.*, vol. 7, no. 3,pp. 412-432, March1998.

[5] J. Weickert, " Multiscale texture enhancement, " *Computer analysis of images and patterns*, Lecture notes in. Comp. Science, vol.970, Berlin, pp. 230-237,1995.

[6] Vinayak Dutt, " Statistical analysis of ultrasound echo-envelope ", Ph.D. thesis, Mayo Graduate School, 1995.

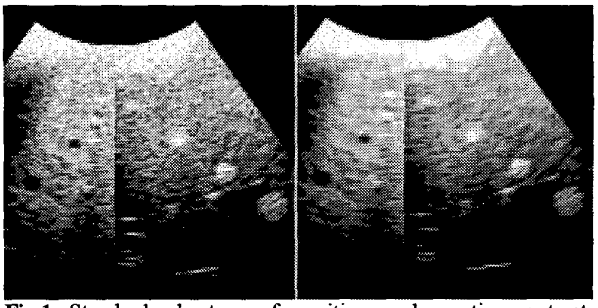

Fig.1 Standard phantom of positive and negative contrast regions. Itr=2, $\Delta t = 2$, $\alpha = 0.9$, s^2=2. (left) original, (right) filtered.

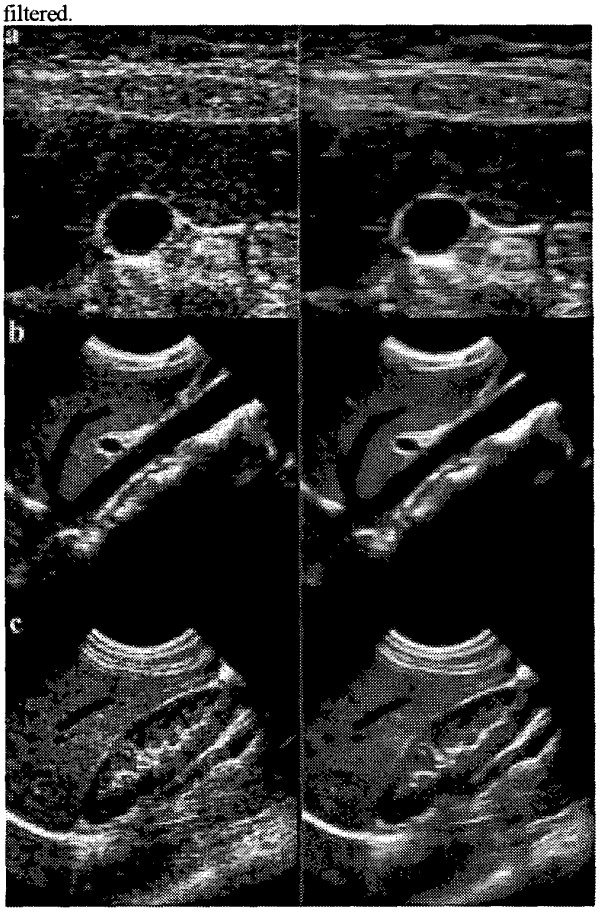

Fig.2 The effect of the algorithm on clinical images (a) abdomen, (b) blood vessels, (c) kidney. Itr=2, $\Delta t = 2$, $\alpha = 0.9$, s^2=2. (left) original, (right) filtered.